High-Temperature Shock Tube Measurements of Dimethyl Ether Decomposition and the Reaction of Dimethyl Ether with OH

Robert D. Cook,* David F. Davidson, and Ronald K. Hanson

Stanford University, Department of Mechanical Engineering, 452 Escondido Mall, Stanford, California 94305

Received: March 17, 2009; Revised Manuscript Received: July 10, 2009

We measured the first high-temperature rate measurements of two dimethyl ether (DME) reactions, (1) DME + Ar → CH_3O + CH_3 + Ar and (2) DME + OH → CH_3OCH_2 + H_2O, in a shock tube by monitoring OH radicals. OH was measured with a narrow-line width laser absorption diagnostic using the well-known $R_1(5)$ line of the A-X(0,0) transition at 306.7 nm. The rate k_1 is in the falloff regime at high temperatures, so it was measured at several pressures from 0.6 to 11.5 atm and temperatures from 1349 to 1790 K. OH radicals were formed by shock-heating mixtures of DME and O_2 in Ar. These mixtures take advantage of the rapid decomposition of the product CH_3O, forming H-atoms, which react with O_2 to form OH. In carefully chosen mixtures, OH concentration is primarily sensitive to k_1 and the well-known rate of H + O_2 → OH + O. Uncertainty in the k_1 measurements was estimated to be ±35%. The rate measurements were then modeled using RRKM theory, which describes the data quite well. Both the rate measurements and the RRKM model were fit from 1000 to 1800 K using the Troe falloff form: $k_{1,\infty}(T) = (4.38 \times 10^{21})T^{-1.57}$ exp(−42 220 K/T) s^{-1}, $k_{1,o} = 7.52 \times 10^{15}$ exp(−21 537 K/T) cm^3 mol^{-1} s^{-1}, and $F_{cent} = 0.454$ exp(−T/2510). The rate of k_2 was measured at pressures near 1.6 atm and temperatures from 923 to 1423 K. OH radicals were generated by the thermal decomposition of the OH precursor *tert*-butyl hydroperoxide (TBHP), and k_2 was inferred from the observed decay of OH with an estimated uncertainty of ±40%. The high-temperature measurements were compared with several rate evaluations and previous low-temperature measurements. The rate evaluation by Curran et al. of $k_2 = (6.32 \times 10^6)T^2$ exp(328 K/T) (cm^3 mol^{-1} s^{-1}) was found to be an excellent fit to both the previous low-temperature measurements and this work.

Introduction

Dimethyl ether (DME, $H_3C-O-CH_3$) has been studied extensively as an alternative fuel or fuel additive in diesel engines because of its ability to reduce pollutant emissions. In addition, biofuels contain many oxygenated species, further motivating the study of detailed oxygenate chemistry. DME is one of the simplest oxygenates and has a significant experimental and modeling database. The earliest studies measured DME pyrolysis in static and flow reactors.[1−4] More recently, flow reactor studies have investigated and developed models for DME oxidation.[5−8] Several previous shock tube studies of DME have been performed. A study by Pfahl et al. examined ignition delay times at high pressures (13 and 40 atm)[9] and a study by Dagaut et al. provided a set of high-temperature ignition delay time data.[10] Also, high-temperature ignition delay times and OH time histories were recently measured in our laboratory.[11] Results from this last study indicated that the rates of k_1 used in most DME oxidation mechanisms were not completely correct, which strongly motivated the current work. A high-temperature shock tube study of DME pyrolysis by Hidaka et al. monitored several decomposition products using lamp absorption at 216 nm and laser absorption at 3.39 μm.[12] On the basis of the results of these studies, several detailed DME oxidation mechanisms have been proposed.[7,8,10] Whereas the detailed mechanisms typically fit a broad set of experimental data, there is significant disagreement on the rates of important reactions. Through the use of an established OH laser absorption diagnostic, we are able to present here rate measurements of two important reactions in the DME oxidation system

$$CH_3OCH_3 + Ar \rightarrow CH_3O + CH_3 + Ar \qquad (1)$$

$$CH_3OCH_3 + OH \rightarrow CH_3OCH_2 + H_2O \qquad (2)$$

The DME decomposition rate (k_1) is one of the most important rates in all DME oxidation and pyrolysis mechanisms. The earliest DME pyrolysis measurements in flow reactors provided the first data for decomposition rates at temperatures below ∼1200 K.[1−4] However, it is very difficult to apply those rates to comprehensive oxidation mechanisms. Because the DME decomposition rate is in the falloff regime under the conditions of the earliest studies, the rate cannot be extrapolated to higher temperatures with a standard Arrhenius rate expression. The previous studies were also performed in several different bath gases (DME, CH_4, N_2) and at several different pressures. Finally, the stated uncertainty in the rate measurements is typically a factor of three. The more recent flow reactor[7,8] and shock tube[9,10,12] studies suggested rates that varied by a factor of two at high temperatures (1200−1700 K) at 1 atm. The RRKM modeling results used in the comprehensive oxidation mechanisms of Curran et al.[7] and Zhao et al.[8] also differ by a factor of two. Direct, high-temperature measurements over a range of pressures in the falloff regime are clearly needed to resolve these differences.

The reaction of DME with OH (k_2) has been measured in several studies at temperatures from 230 to 650 K.[13−18] All of

* Corresponding author. E-mail: robtpt@stanford.edu.

10.1021/jp902403n CCC: $40.75
Published on Web 08/20/2009

the previous studies were performed in flow reactors, and OH radicals were generated using photolysis methods. OH was monitored in the previous studies by laser-induced fluorescence (LIF)[15−18] or the fluorescence of OH excited by lamps.[13,14] In all cases, mixtures were chosen to produce the pseudo-first-order decay of OH radicals. The LIF studies agree well within experimental uncertainties. The lamp studies disagree somewhat compared with the others, with one study[13] slightly higher than the others and one study[14] slightly lower. The rates used in the detailed mechanisms of Curran et al.[7] and Zhao et al.[8] agree very well with the previous experimental data at low temperatures but differ by about 30% at 1400 K. The rate used by Dagaut et al. is significantly lower.[10] Because this rate is important at high temperatures in DME oxidation and there is significant pre-exponential temperature dependence, it is important to provide direct rate measurements at high temperatures.

In this study, the rates k_1 and k_2 were measured behind reflected shock waves using narrow-line width laser absorption of OH radicals at 306.7 nm. The rate k_2 was measured directly using *tert*-butyl hydroperoxide (TBHP) as an OH precursor at pressures of 1.9 and 1.2 atm and temperatures from 923 to 1423 K. Highly sensitive measurements of k_1 were performed in very dilute mixtures of DME/O_2/Ar at pressures from 0.6 to 11.5 atm and temperatures from 1349 to 1790 K. Calculations of the rate k_1 based on RRKM/master equation modeling were also performed and compared with the measurements.

Experimental Setup

All experiments were performed behind reflected shock waves in a high-purity, 15 cm diameter, helium-driven, stainless steel shock tube. Optical measurements were made at a location 2 cm from the endwall of the shock tube. Incident shock velocity is calculated on the basis of five piezoelectric pressure transducer measurements spread over the last 2 m of the shock tube and linearly extrapolated to the endwall. Temperature and pressure in the reflected shock region are calculated using a frozen chemistry ideal shock code, resulting in an uncertainty of <1% in the initial temperature.

Mixtures were prepared manometrically in a high-purity mixing assembly and stored in a 14 L stainless steel mixing vessel. A magnetically driven stirrer was used to ensure homogeneous mixtures. Details of the methods used in our laboratory to prepare accurate mixtures have been reported elsewhere.[19] Research grade Ar (99.999%), O_2 (99.999%), and He (99.999%) were supplied by Praxair. DME (99+%) and a 70% solution of *tert*-butyl hydroperoxide (used as an OH precursor) in water were supplied by Sigma-Aldrich. Between experiments, the shock tube and mixing manifold were routinely pumped down to $\sim 3 \times 10^{-6}$ and $\sim 10^{-3}$ torr, respectively, to ensure the purity of the test mixture. The leak-plus-outgassing rate was $\sim 5 \times 10^{-6}$ torr/min.

OH concentration was measured using narrow-line width laser absorption near 306.7 nm. The chosen OH wavelength was the peak of the well-characterized $R_1(5)$ absorption line in the OH A-X (0,0) band. Laser light at 613.4 nm was generated by a Spectra Physics 380 dye laser pumped by a 5W Coherent Verdi at 532 nm. Light at 306.7 nm was generated by intracavity frequency-doubling, using a temperature-tuned AD*A crystal. Common mode rejection was used to reduce laser intensity noise to <0.1%, resulting in a minimum detection sensitivity of <1 ppm for most conditions in this work. OH concentration was calculated using Beer's law, and the estimated uncertainty in measured X_{OH} is ~3%. Measurements were also performed with the laser tuned off the OH absorption line and with the laser turned off to verify that there was no significant interfering absorption or emission. Further details of the OH laser absorption diagnostic are available elsewhere.[20]

Results

DME + Ar → CH_3O + CH_3 + Ar Rate Measurement. We measured the DME decomposition rate (k_1) by monitoring OH radicals behind reflected shock waves at $P = 0.6$, 1.5, 4.3, and 11.4 atm and at temperatures from 1349 to 1790 K. The formation rate of OH was always dependent on the well-known H + O_2 chain branching reaction. However, OH formation was also very sensitive to the DME decomposition rate, and with the proper selection of mixtures, sensitivity to other interfering reactions was minimized. We minimized interference by making mixtures with very little DME in excess O_2. This method has been previously used with success in this laboratory to measure the rate of CH_2O + M.[21] In the case of DME, the formation of OH follows this path

Step 1:

$$\text{DME} \rightarrow \text{CH}_3\text{O} + \text{CH}_3 \quad \text{(target rate)}$$

Step 2:

$$\text{CH}_3\text{O} \rightarrow \text{CH}_2\text{O} + \text{H} \quad \text{(fast)}$$

Step 3:

$$\text{H} + \text{O}_2 \rightarrow \text{OH} + \text{O} \quad \text{(well-known)}$$

For clarity, in addition to k_1 and k_2 (defined previously), the following two reactions are numbered k_3 and k_4

$$\text{CH}_3\text{O} \rightarrow \text{CH}_2\text{O} + \text{H} \tag{3}$$

$$\text{H} + \text{O}_2 \rightarrow \text{OH} + \text{O} \tag{4}$$

Because step 2 is nearly instantaneous above 1300 K, OH is primarily sensitive to the target rate and the rate of H + O_2 (k_4). However, whereas the H + O_2 chain branching rate (k_4) is very well-characterized, with an uncertainty of only about 9% over the temperature range in this study,[22] the Curran et al.[7] mechanism uses a rate similar to the one reported in 1992 by Baulch et al.[23] That rate is about 15% higher than the rate used in the Zhao et al.[8] mechanism and 25% higher than the GRI 3.0 rate[24] at the highest temperatures in this study. Therefore, the DME oxidation model of Curran et al.[7] was modified to include the GRI 3.0 rate[24] for k_4 in this analysis. Sensitivity analysis based on the updated Curran et al.[7] model was performed, confirming that k_1 and k_4 are dominant if the mixture is chosen carefully (Figure 1). Sensitivity was also calculated using the model of Curran et al.[7] that was further updated with the value for k_1 measured here and calculated on the basis of the unmodified mechanism of Zhao et al.[8] All three sensitivity calculations resulted in similar isolation of k_1 and k_4. In this work, sensitivity is defined as $(dX_{OH}/dk_i)/(k_i/X_{OH})$, where X_{OH} is the local OH mole fraction and k_i is the rate coefficient of reaction i. The rate k_1 was inferred by matching measured and modeled OH over the appropriate time frame (Figure 2), ranging from the first 25 μs at higher temperatures to about 150 μs at the lowest temperatures in this study. All rate measurements are listed in Table 1. The data reported here are based on the model of Curran et al.[7] using the GRI 3.0 rate for k_4. To verify that the rate determination method is robust, we also determined

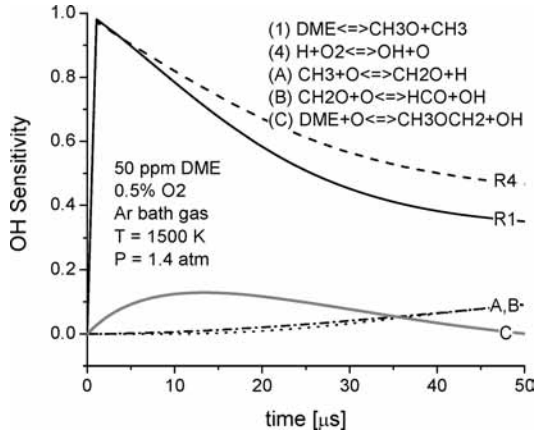

Figure 1. OH sensitivity plot for rate measurement of DME + Ar ↔ $CH_3O + CH_3 + Ar$.

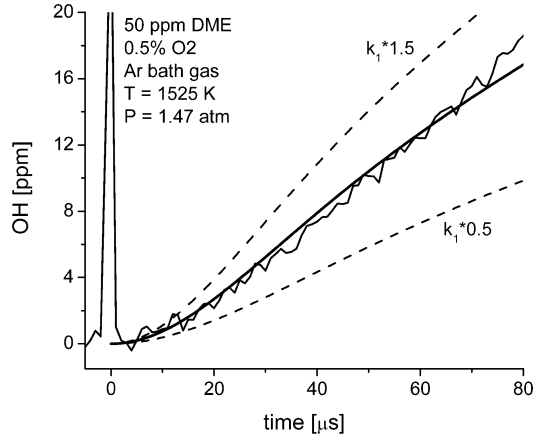

Figure 2. Example DME decomposition rate measurement. The solid line is fit to the data by adjusting k_1, whereas the dashed lines show the best fit of $k_1 \pm 50\%$.

TABLE 1: DME + Ar → $CH_3O + CH_3$ + Ar Rate Data

50 ppm DME, 0.5% O_2 in Ar			30 ppm DME, 0.3% O_2 in Ar		
T (K)	P (atm)	k (1/s)	T (K)	P (atm)	k (1/s)
1379	0.692	550	1459	1.470	2500
1455	0.663	1900	1494	1.488	4000
1555	0.631	7000	1572	1.456	12 000
1665	0.568	18 000	1621	1.429	18 000
1786	0.518	47 000	1668	1.412	29 000
1349	1.591	550	1718	1.426	40 000
1375	1.593	900	1728	1.391	40 000
1379	1.516	900	1743	1.371	49 000
1425	1.552	1600	1352	4.529	750
1453	1.503	2600	1442	4.468	3600
1525	1.470	7500	1553	4.352	15 500
			1665	4.105	58 000
			1790	4.002	150 000
			1349	12.19	900
			1453	11.70	6100
			1580	11.03	27 000
			1653	10.48	75 000

the rate of k_1 by adjusting its rate in the unmodified mechanism of Zhao et al.[8] The difference in the rates derived from these two methods was always less than 10% and usually less than 5%. The effect of the updated value for k_2 (discussed in the next section) was also examined, and it had no significant impact on the k_1 rate determination. A detailed error analysis, including uncertainty in temperature, pressure, mixture composition, data fitting, OH absorption coefficient calculation, wavemeter reading, and the rates of the ten most important secondary reactions

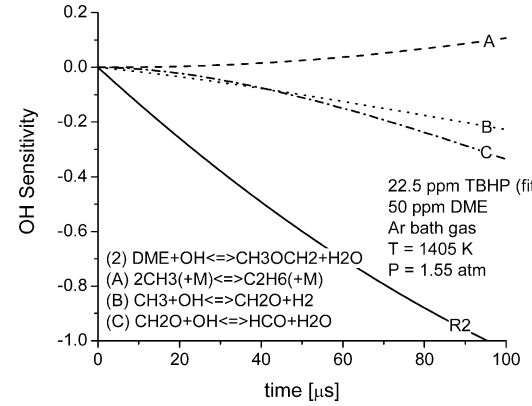

Figure 3. OH sensitivity plot for rate measurement of DME + OH ↔ $CH_3OCH_2 + H_2O$.

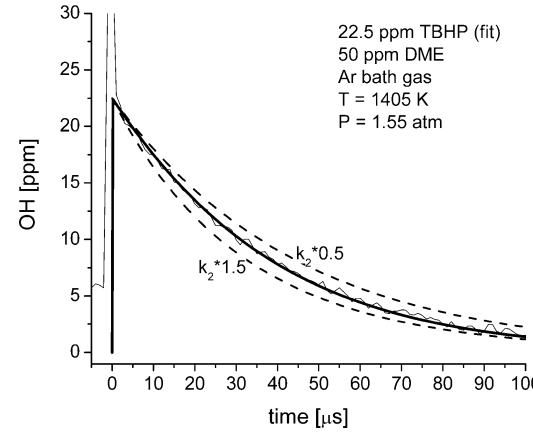

Figure 4. Example DME + OH rate measurement. The solid line is fit to the data by adjusting k_2 and initial TBHP, whereas the dashed lines show the best fit of $k_2 \pm 50\%$.

was also performed, resulting in an estimated measurement uncertainty of ±35% for k_1.

DME + OH → $CH_3OCH_2 + H_2O$ Rate Measurement. We measured the rate of DME + OH (k_2) by monitoring the decay of OH radicals behind reflected shock waves at pressures near 1.4 atm and temperatures from 923 to 1470 K. OH radicals were produced by the rapid thermal decomposition of TBHP in the reflected shock region.[24] Decomposition of TBHP yields an OH radical, a CH_3 radical, and acetone as follows

$$(CH_3)_3\text{-CO-OH} \rightarrow (CH_3)_3\text{-CO} + OH \quad (5)$$

$$(CH_3)_3\text{-CO} \rightarrow CH_3COCH_3 + CH_3 \quad (6)$$

In mixtures of DME and TBHP in Ar, the decay of OH radicals is primarily sensitive to k_2, with very little interference from other reactions. Experimental data were modeled by the DME oxidation mechanism of Curran et al.,[7] edited to include reactions 5 and 6. Sensitivity analysis was also performed for all experiments (Figure 3). At higher temperatures, OH is primarily sensitive to the targeted reaction (k_2), although at lower temperatures, OH is also sensitive to the rate k_5 at very early times. However, k_5 has recently been measured directly with an uncertainty of ±25%[25] and does not significantly impact the measurements in this study. An example data trace showing the rate determination of k_2 is shown in Figure 4. Several different mixtures were considered with initial TBHP concentration varying from 10 to 30 ppm and initial DME concentration

TABLE 2: DME + OH ↔ CH_3OCH_2 + H_2O Rate Data

T (K)	P (atm)	k (cm^3 mol^{-1} s^{-1})
	200 ppm DME, ~30 ppm TBHP in Ar	
947	2.071	9.00×10^{12}
1055	1.886	1.15×10^{13}
1105	1.815	1.29×10^{13}
	50 ppm DME, ~30 ppm TBHP in Ar	
969	1.990	1.05×10^{13}
1015	1.957	1.10×10^{13}
1103	1.806	1.35×10^{13}
1181	1.779	1.60×10^{13}
	50 ppm DME, ~15 ppm TBHP in Ar	
1139	1.789	1.50×10^{13}
1207	1.739	1.55×10^{13}
1237	1.697	1.55×10^{13}
1271	1.669	1.70×10^{13}
1311	1.643	1.80×10^{13}
1372	1.623	1.90×10^{13}
	50 ppm DME, ~22.5 ppm TBHP in Ar	
1039	1.936	1.15×10^{13}
1067	1.888	1.15×10^{13}
1338	1.624	1.65×10^{13}
1405	1.552	2.02×10^{13}
1420	1.544	1.90×10^{13}
1470	1.525	2.05×10^{13}
	pseudo-first-order data	
	250 ppm DME, ~15 ppm TBHP in Ar	
923	1.415	8.02×10^{12}
992	1.421	1.10×10^{13}
1037	1.382	1.14×10^{13}
1089	1.340	1.21×10^{13}
1141	1.333	1.38×10^{13}
1218	1.218	1.56×10^{13}
1323	1.236	1.81×10^{13}
1343	1.144	1.84×10^{13}
1423	1.111	2.10×10^{13}

varying from 50 to 250 ppm. Because wall adsorption and condensation of TBHP was observed, initial TBHP mole fraction had to be inferred from the OH data. OH decays rapidly behind the reflected shock, so the inferred initial TBHP mole fraction is a significant source of experimental uncertainty. Two mixtures in which $[DME]_0/[TBHP]_0 = 17$ were also prepared. In these mixtures, OH decayed under pseudo-first-order conditions, which allowed the rate k_2 to be measured without sensitivity to the initial TBHP mole fraction. In the pseudo-first-order mixtures, we determined k_2 by measuring the slope of log[OH] versus time (insensitive to initial TBHP) and also by adjusting k_2 to fit the quantitative OH data. The two methods for determining k_2 differ by no more than 10%, although the rate data do display significantly less scatter when sensitivity to initial TBHP concentration is eliminated. All rate data for k_2 are listed in Table 2. A detailed error analysis, including uncertainty in temperature, pressure, mixture composition, data fitting, initial TBHP concentration, OH absorption coefficient calculation, wavemeter reading, and the rates of the five most important interfering reactions was also performed, resulting in an estimated overall measurement uncertainty of ±40%. Similar analysis of the data fit by the pseudo-first-order method resulted in a slightly lower uncertainty of ±35%.

RRKM Modeling of DME Decomposition. The DME decomposition rate was modeled using single-channel RRKM/1-D master equation calculations using the Multiwell code by Barker et al.[26,27] The DME transition state was selected using the hindered Gorin model.[28] The C−O bond length of the transition state was increased using the Lennard-Jones

TABLE 3: List of Parameters Used in RRKM Model

barrier height (0 K)	81.1 kcal/mol
	CH_3OCH_3
moments of inertia (amu Å^2)	2-D: 53.5; 1-D: 12.9
symmetry	2
vibrational frequencies (cm^{-1})	2156, 242, 399, 920, 1091, 1128, 1162, 1167, 1229, 1425, 1450, 1457, 1458, 1467, 1488, 2855, 2870, 2900, 2904, 3008, 3010
	$CH_3O\cdots CH_3$
moments of inertia (amu Å^2)	2-D: 171.2; 1-D: 17.7
symmetry	1
vibrational frequencies (cm^{-1})	712, 941, 1803, 1344, 1345, 1488, 2803, 2868, 2904, 3184(2), 3002, 1383(2), 580
CH_3 2-D internal rotor (amu Å^2)	1.78, $\eta = 0.94$
CH_3O 2-D internal rotor (amu Å^2)	18.2, $\eta = 0.94$

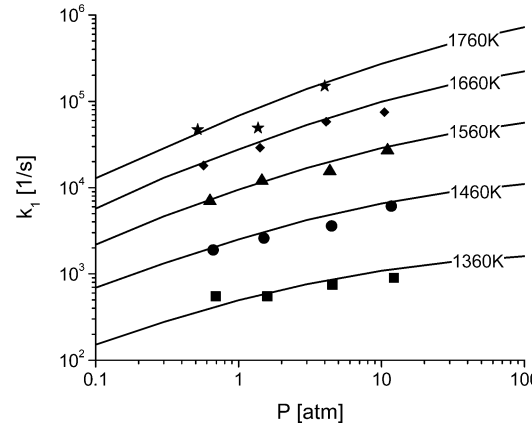

Figure 5. Falloff plot comparing current data (symbols) for k_1 with the RRKM model (lines) near five different temperatures (±15 K).

form of the potential, such that $r^{\ddagger}/r = (6D_0/RT)^{1/6}$, and the resulting molecule was treated as an approximately symmetric top. Transition-state vibrational frequencies are assumed to be those of the CH_3O and CH_3 fragments as well as their internal rotations. The 2-D internal rotors were adjusted by a hindrance parameter, η, such that $I^{\ddagger} = I(1 - \eta)^{1/2}$. Values for the hindrance parameter were chosen to fit the high-pressure limit rate calculations by Zhao et al.[8] In that study, the high-pressure limit was calculated by assuming a constant value of 2.75×10^{13} cm^3 mol^{-1} s^{-1} for the reverse rate. The result was that η had an approximately constant value of 0.94 over the temperature range of this study, although it does fall off to lower values below 1000 K. Lennard-Jones parameters for DME and Ar were taken from refs 26 and 29; vibrational frequencies and moments of inertia for DME and CH_3O were taken from ref 8, and those for CH_3 were taken from ref 30; and barrier height was taken from ref 31. All values used in this work are listed in Table 3.

An exponential-down collisional energy transfer model was used to fit the experimental data in this study. No systematic temperature dependence of the value for ΔE_{down} was observed, and a value of $\Delta E_{down} = 550$ cm^{-1} was found to be the best fit. Using the model presented here, a falloff plot (Figure 5) and an Arrhenius plot (Figure 6) were generated, showing good agreement between our calculated and measured rates. Using the RRKM model, values for F_{cent} in the well-known Troe falloff format were calculated in the temperature range from 1200 to 2000 K. The following rate expression results in excellent agreement with both the measurements and the RRKM model presented here

$$k_{1,\infty}(T) = (4.38 \times 10^{21})T^{-1.57} \exp(-42\,220\ \mathrm{K}/T)\ \mathrm{s}^{-1}$$

$$k_{1,o} = (7.52 \times 10^{15}) \exp(-21\,537\ \mathrm{K}/T)\ \mathrm{cm}^3\ \mathrm{mol}^{-1}\ \mathrm{s}^{-1}$$

$$F_{cent} = 0.454 \exp(-T/2510)$$

Discussion

Whereas the rate k_1 has not previously been measured directly at high temperatures, several rate calculations and fits have been carried out to model DME oxidation and pyrolysis data.[7,8,10,12] A selected group of these rates has been plotted and compared with the measured rate data and RRKM modeling at $P = 1.5$ atm in Figure 7. The measurements from the current study are closer to the calculated pressure-dependent rate of Curran et al.[7] at the lower temperatures but are closer to the calculated pressure-dependent rate of Zhao et al.[8] at the higher temperatures. In addition, the measurements in this study exhibit significantly stronger pre-exponential temperature dependence than any of the previous calculations or fits. However, our RRKM modeling results also show stronger pre-exponential temperature dependence than previous calculations and fit all of our measured data reasonably well (Figures 6 and 7). The largest discrepancy between the measured and modeled rates occurs at the highest temperatures at $P = 1.5$ atm, but the maximum deviation is ~30%, which is within the estimated uncertainty of 35% in the measurements. The current experimental and modeled rates also fall between the decomposition

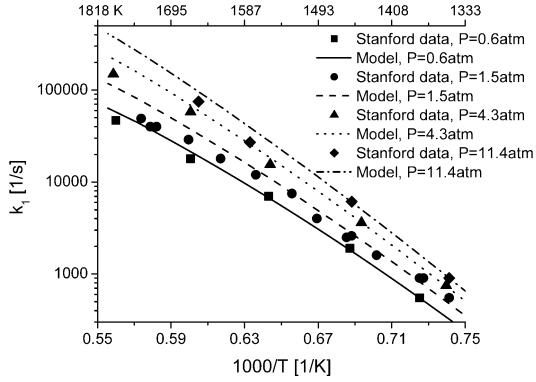

Figure 6. Arrhenius plot comparing current data (symbols) for k_1 with the RRKM model (lines) at four different pressures.

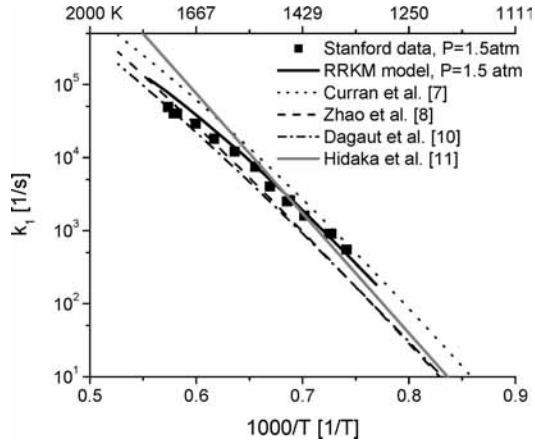

Figure 7. Comparison of measured k_1 rate and RRKM model (current study) with previous rate calculations[7,8,10] and fit to shock tube pyrolysis data[12] at $P = 1.5$ atm.

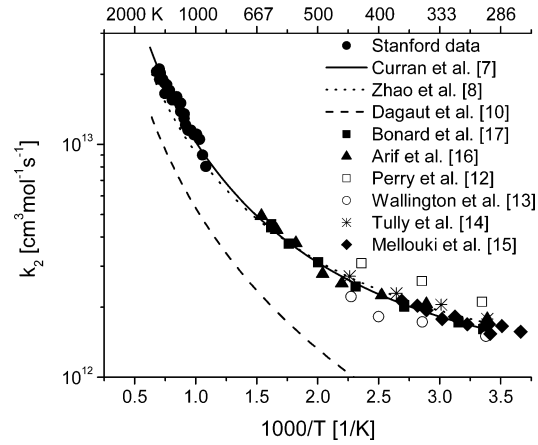

Figure 8. Comparison of measured high-temperature k_2 rate with rates used in DME mechanisms (lines), low-temperature LIF measurements (solid symbols), and low-temperature fluorescence measurements (open symbols).

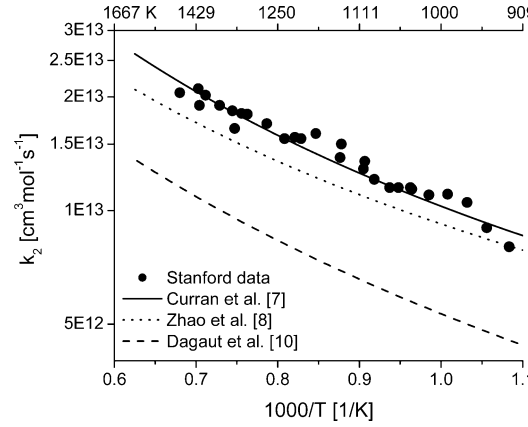

Figure 9. Comparison of measured high-temperature k_2 rate to rates used in the DME mechanisms (lines).

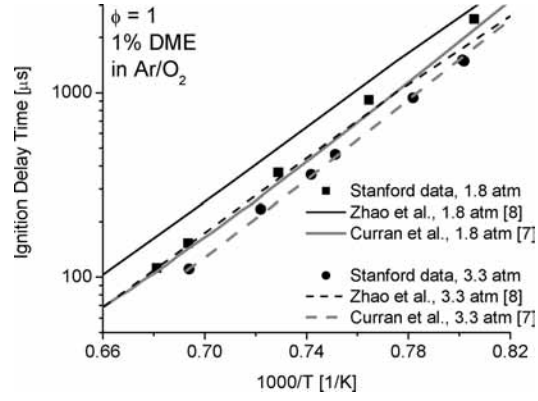

Figure 10. Comparison of measured DME ignition delay times with the oxidation mechanisms of Zhao et al.[8] and Curran et al.[7]

rates used by the two most recent and comprehensive studies of high-temperature DME oxidation.[7,8]

The measured rate k_2 is compared with previous data and rate evaluations over a broad range of temperatures in Figure 8. The fitted rates used by Curran et al.[7] and Zhao et al.[8] both reconcile the previous low-temperature rate measurements and the high-temperature rate measurements presented here. However, the rate used by Dagaut et al.[10] is too low by a factor of two at high temperatures and by a factor of four at low temperatures. Figure 9 is a comparison of this work and the rate evaluations at high temperatures, showing that

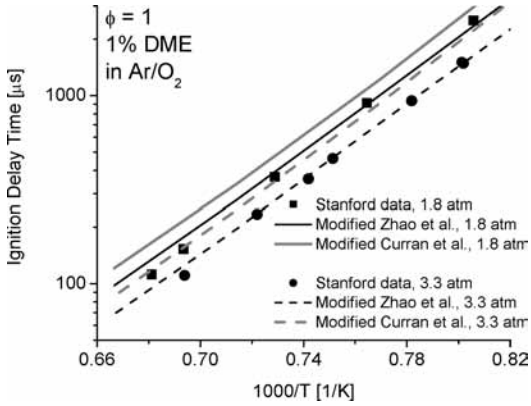

Figure 11. Comparison of measured DME ignition delay times with modified oxidation mechanisms.

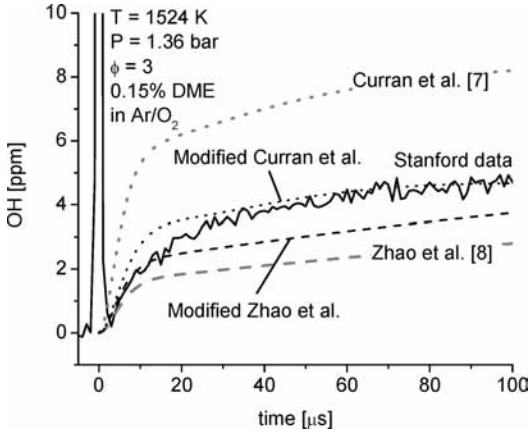

Figure 12. Comparison of measured OH time histories with modified and unmodified DME oxidation mechanisms at $T = 1524$ K.

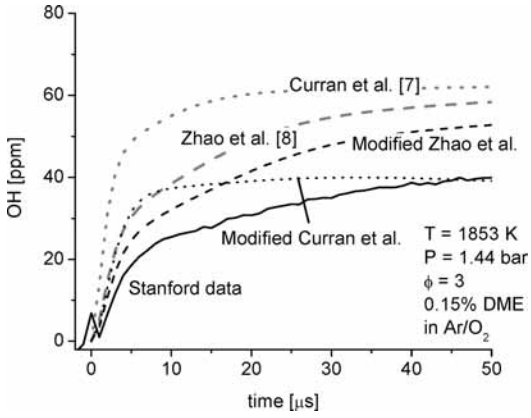

Figure 13. Comparison of measured OH time histories with modified and unmodified DME oxidation mechanisms at $T = 1853$ K.

the new high-temperature measurements tend to favor the evaluation of Curran et al.,[7] although the Zhao et al.[8] rate is only 30% lower at 1400 K, which is within the estimated 40% uncertainty of this study.

The measured DME decomposition rate (k_1) has also been incorporated into the recent mechanisms by Curran et al.[7] and Zhao et al.[8] and compared with the recent study performed in our laboratory.[11] The mechanisms are in good agreement with the rate of k_2, and both agree reasonably well with the rate measurement presented here. However, the mechanisms differ significantly on two extremely important rates. As previously stated, the values used for the DME decomposition rate (k_1) differ by about a factor of two at high temperatures, and both rates disagree significantly with our rate measurement. The modified mechanisms presented here are both updated with the newly measured pressure-dependent DME decomposition rate, and the mechanism of Curran et al.[7] is also updated with the GRI 3.0 rate[24] for

$$H + O_2 \rightarrow OH + O$$

Ignition delay times of DME mixtures have recently been measured under a broad range of conditions.[11] The original mechanism of Curran et al.[7] reproduces high-temperature ignition delay times extremely well, whereas the original mechanism of Zhao et al.[8] predicts ignition delay times that are 10−40% longer than the measurements (Figure 10). The modified Curran et al.[7] mechanism predicts ignition delay times that are 15−30% longer than the measurements, whereas the modified mechanism of Zhao et al.[8] is much improved and agrees with the measured ignition delay times extremely well. The results of the updated mechanisms are shown in Figure 11.

OH time histories in rich DME oxidation have also been measured recently in this laboratory.[11] Comparisons between measured OH and the modified and unmodified DME oxidation mechanisms at $T = 1524$ K are shown in Figure 12. The unmodified mechanism of Curran et al.[7] predicts OH profiles that are significantly higher than the measurement, whereas the unmodified mechanism of Zhao et al.[8] predicts OH profiles that are significantly lower than the measurement. However, agreement between modeled and measured OH is improved in both modified mechanisms. Figure 13 shows the performance of the modified and unmodified mechanisms at a higher $T = 1853$ K. Under this condition, both unmodified mechanisms greatly overpredict OH. The modified mechanisms are both improved and the modified Zhao et al.[8] mechanism performs somewhat better at short times, whereas the modified Curran et al.[7] mechanism provides better agreement at long times.

Conclusions

A narrow line width laser absorption diagnostic for measuring OH radicals was used to make measurements of DME decomposition (k_1) and the first high-temperature measurements of DME + OH (k_2). The rate k_1 was measured at four pressures, $P = 0.6$, 1.5, 4.3, and 11.4 atm, and at temperatures from 1349 to 1790 K. RRKM/master equation rate calculations were carried out and resulted in very good agreement over the entire range of experimental data. The high-temperature rate measurements of k_2 verified that the pre-exponential temperature dependence of $\sim T^2$, which is used in several comprehensive DME oxidation mechanisms, is essentially correct and agreed extremely well with the rate evaluations of both Curran et al.[7] and Zhao et al.[8] Finally, the mechanisms of Curran et al.[7] and Zhao et al.[8] were modified on the basis of the new rate measurements and compared with previous work done in this laboratory.[11]

Acknowledgment. This work was sponsored by the Global Climate and Energy Project (GCEP) and the Department of Energy, with Drs. Larry Rahn and Wade Sisk as contract monitors. We also thank Dr. David Golden (Stanford University) for helpful discussions about RRKM modeling.

References and Notes

(1) Pacey, P. D. *Can. J. Chem.* **1975**, *53*, 2742.
(2) Aronowitz, D.; Naegeli, D. *Int. J. Chem. Kinet.* **1977**, *9*, 471.

(3) Batt, L.; Alvarado-Salinas, G.; Reid, I. A. B.; Robinson, C.; Smith, D. B. *Proc. Combust. Inst.* **1982**, *19*, 81.
(4) Held, A. M.; Manthorne, K. C.; Pacey, P. D.; Reinholdt, H. P. *Can. J. Chem.* **1977**, *55*, 4128.
(5) Curran, H. J.; Pitz, W. J.; Westbrook, C. K.; Dagaut, P.; Boettner, J. C.; Cathonnet, M. *Int. J. Chem. Kinet.* **1998**, *30*, 229.
(6) Fischer, S. L.; Dryer, F. L.; Curran, H. J. *Int. J. Chem. Kinet.* **2000**, *32*, 713.
(7) Curran, H. J.; Fischer, S. L.; Dryer, F. L. *Int. J. Chem. Kinet.* **2000**, *32*, 741.
(8) Zhao, Z.; Chaos, M.; Kazakov, A.; Dryer, F. L. *Int. J. Chem. Kinet.* **2008**, *40*, 1.
(9) Pfahl, U.; Fieweger, K.; Adomeit, G. *Proc. Combust. Inst.* **1996**, *26*, 781.
(10) Dagaut, P.; Daly, C.; Simmie, J. M.; Cathonnet, M. *Proc. Combust. Inst.* **1998**, *27*, 361.
(11) Cook, R. D.; Davidson, D. F.; Hanson, R. K. *Proc. Combust. Inst.* **2009**, *32*, 189.
(12) Hidaka, Y.; Sato, K.; Yamane, M. *Combust. Flame* **2000**, *123*, 1.
(13) Perry, R. A.; Atkinson, R.; Pitts, J. N. *J. Chem. Phys.* **1977**, *67*, 611.
(14) Wallington, T. J.; Liu, R.; Dagaut, P.; Kurylo, M. J. *Int. J. Chem. Kinet.* **1998**, *20*, 41.
(15) Tully, F. P.; Droege, A. T. *Int. J. Chem. Kinet.* **1987**, *19*, 251.
(16) Mellouki, A.; Teton, S.; le Bras, G. *Int. J. Chem. Kinet.* **1995**, *27*, 791.
(17) Arif, M.; Dellinger, B.; Taylor, P. H. *J. Phys. Chem. A* **2000**, *101*, 2436.
(18) Bonard, A.; Daele, V.; Delfau, J.; Vovelle, C. *J. Phys. Chem. A* **2002**, *106*, 4385.
(19) Horning, D. C.; Davidson, D. F.; Hanson, R. K. *J. Propul. Power* **2002**, *18*, 363.
(20) Herbon, J. T.; Hanson, R. K.; Golden, D. M.; Bowman, C. T. *Proc. Combust. Inst.* **2002**, *29*, 1201.
(21) Vasudevan, V. V.; Davidson, D. F.; Hanson, R. K.; Bowman, C. T.; Golden, D. M. *Proc. Combust. Inst.* **2007**, *31*, 175.
(22) Yu, C. L.; Frenklach, M.; Masten, D. A.; Hanson, R. K.; Bowman, C. T. *J. Phys. Chem.* **1994**, *98*, 4770.
(23) Baulch, D. L.; Cobos, C. J.; Cox, R. A.; Esser, C.; Frank, P.; Hayman, G.; Just, T.; Kerr, J. A.; Pilling, M. J.; Troe, J.; Walker, R. W.; Warnatz, J. *J. Phys. Chem. Ref. Data* **1992**, *21*, 411.
(24) Smith, G. P.; Golden, D. M.; Frenklach, M.; Moriarty, N. W.; Eitneer, B.; Goldenberg, M.; Bowman, C. T.; Hanson, R. K.; Song, S., Jr.; Lissianski, V. V.; Qin, Z. GRI-Mech Home Page. http://www.me.berkeley.edu/gri_mech/ (accessed Jul 2009).
(25) Vasudevan, V.; Davidson, D. F.; Hanson, R. K. *Int. J. Chem. Kinet.* **2005**, *37*, 98.
(26) Barker, J. R.; Ortiz, N. F.; Preses, J. M.; Lohr, L. L. *MultiWell-2008.3 Software*. http://aoss.engin.umich.edu/multiwell (accessed Jun 2008).
(27) Barker, J. R. *Int. J. Chem. Kinet.* **2001**, *33*, 232.
(28) Smith, G. P.; Manion, J. A.; Rossi, M. J.; Rodgers, A. S.; Golden, D. M. *Int. J. Chem. Kinet.* **1994**, *26*, 211.
(29) Reid, R. C.; Prausnitz, J. M.; Poling, B. E. *The Properties of Gases and Liquids*, 4th ed.; McGraw-Hill Book Company: New York, 1987.
(30) Eng, R. A.; Gebert, A.; Goos, E.; Hippler, H.; Kachiani, C. *Phys. Chem. Chem. Phys.* **2001**, *3*, 2258.
(31) Benson, S. W. *J. Chem. Phys.* **1956**, *25*, 27.

JP902403N